

## The sedimentation of a small particle through a fluid-filled pore of finite length

R. SHAIL and I.M. WARRILOW

*Department of Mathematics, University of Surrey, Guildford, Surrey, GU2 5XH, UK*

Received 4 January 1988; accepted 22 February 1988

**Abstract.** This paper investigates the axisymmetric sedimentation of a small slowly rotating and translating particle through a fluid-filled circular pore of finite length which communicates with two half-space chambers of fluid. In the quasi-steady Stokes approximation the particle is modelled by either a rotlet or Stokeslet, and potential-theoretic methods are used to reduce each problem to the solution of coupled infinite systems of linear equations. The numerical solutions of these sets of equations are used to compute approximations to the resistive torque and drag experienced by the particle.

### 1. Introduction

In a recent paper Shail and Packham [1] have considered a class of axisymmetric problems in which a rotating or translating particle sediments from a half-space of fluid into a semi-infinite circular fluid-filled pore. The particle, which is assumed to be small compared with the pore radius, is modelled by either a rotlet or a Stokeslet, and the fluid motion is assumed to be sufficiently slow to permit the quasi-steady Stokes linearization of the equation of motion. Using potential-theoretic methods the rotlet and Stokeslet problems were reduced to the solution of infinite sets of simultaneous linear equations in the coefficients in eigenfunction expansions of potential functions pertaining to the pore region. These sets of equations were solved by the method of truncation, and a knowledge of the coefficients allows the derivation of approximations to the drag and couple experienced by the particle using formulae due to Brenner [2]. The semi-infinite pore configuration thus complements the model proposed by Davis et al. [3] in which the membrane containing the pore is assumed to be infinitely thin.

The purpose of this paper is to report the results of calculations in which the pore is of finite non-zero length. Thus the basic hydrodynamic configuration consists of two half-spaces of fluid connected together by a fluid-filled circular cylinder of finite length  $2l$ . The slowly sedimenting particle is modelled by a rotlet or Stokeslet placed on the axis of symmetry of the pore, either in one of the half-space chambers of fluid or within the pore. The velocity and potential representations of [1] are extended to account for the presence of a third fluid region, and the solution of the relevant potential problems is again reduced, using the procedures developed in [1], to the consideration of infinite systems of simultaneous linear equations. The numerical solution of these equations, by truncation, then allows the computation of illustrative results for the variation of the torque and drag factors as functions of pore length and the distance of the sedimenting particle from a membrane face.

An outline of the paper is as follows. In Section 2 the rotlet problem is formulated and solved, numerical results being given in graphical form for the torque factor in Brenner's

formula [2] for the resistive couple. In Section 3 we investigate the problem wherein the rotlet is replaced by an axial Stokeslet, there being also a pressure driven flux  $M$  of fluid through the pore. The end-product of this analysis is four infinite sets of simultaneous linear equations for the expansion coefficients in various potential functions. The solution by truncation of these sets of equations is used in Section 4 to compute the drag factor appropriate to a particle sedimenting in a fluid with zero bulk flow. To take account of the effect on the drag of a pressure-driven bulk flow it is necessary to solve a subsidiary singularity-free problem in which the flow results from a pressure difference at infinity between the half-space chambers of fluid. This situation was first considered by Dagan et al. [4] and Section 4 concludes with an alternative formulation in which only half the number of expansion coefficients are needed. Numerical results are presented for the pressure difference at infinity as a function of pore length for unit flux, and the axial fluid speed, which appears in the drag formula [2], is computed.

**2. Basic equations and the rotlet problem**

Let  $(\rho, \theta, z)$  denote cylindrical polar conditions with origin  $O$ . A membrane with impenetrable walls of thickness  $2l$  contains a circular cylindrical pore of unit radius, whose generators are perpendicular to the parallel plane faces of the membrane (see Fig. 1). The origin  $O$  is located at the point where the pore axis intersects one of the plane faces, a choice which enables a comparison with the semi-infinite pore solution ( $l \rightarrow \infty$ ) to be made readily. Viscous incompressible fluid occupies the half-space chambers  $z > 0$  (region I),  $z < -2l$  (region III) and the pore (region II)  $-2l \leq z \leq 0$ ,  $0 \leq \rho \leq 1$ ,  $0 \leq \theta < 2\pi$ . An axisymmetric fluid motion is generated by a point singularity located on the axis of the pore, and for sufficiently small Reynolds numbers the velocity field  $\mathbf{v}$  satisfies the linearized Navier-Stokes and continuity equations

$$\mu \text{curl curl } \mathbf{v} = -\nabla p, \tag{2.1}$$

$$\text{div } \mathbf{v} = 0, \tag{2.2}$$

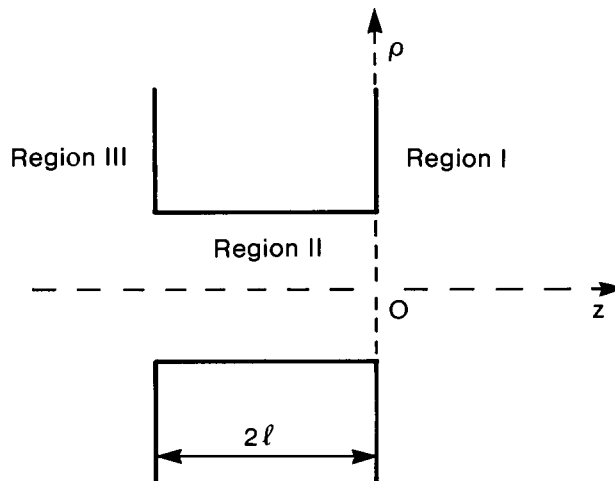


*Fig. 1. The pore-membrane geometry.*

where  $p$  is the dynamic pressure and  $\mu$  the coefficient of viscosity.  $\mathbf{v}$  must also comply with the no-slip condition on the membrane and pore walls.

Suppose now that the singularity is a rotlet of unit strength placed on the axis of symmetry at  $z = h (> 0)$  in region I, and oriented parallel to the  $z$ -axis. In the slow-flow approximation the streamlines are circles lying in planes perpendicular to  $Oz$ , and  $\mathbf{v}$  has a non-zero component  $v(\varrho, z)$  in the  $\theta$ -direction only. Since  $v$  is independent of  $\theta$ , the continuity equation (2.2) is satisfied identically and (2.1) implies the constancy of  $p$  throughout the fluid. Further from (2.1)  $v$  satisfies the equation

$$\frac{\partial^2 v}{\partial \varrho^2} + \frac{1}{\varrho} \frac{\partial v}{\partial \varrho} - \frac{v}{\varrho^2} + \frac{\partial^2 v}{\partial z^2} = 0, \tag{2.3}$$

implying that  $v \cos \theta$  is a harmonic function.

Denote by  $v^I(\varrho, z)$ ,  $v^{II}(\varrho, z)$  and  $v^{III}(\varrho, z)$  the transverse velocity components in the fluid regions I, II and III. As in [1] we write

$$v^I(\varrho, z) = \frac{\varrho}{R_1^3} - \frac{\varrho}{R_2^3} + v_1(\varrho, z), \tag{2.4}$$

where  $R_1 = [\varrho^2 + (z - h)^2]^{1/2}$ ,  $R_2 = [\varrho^2 + (z + h)^2]^{1/2}$ , and the second term in (2.4) is an antiparallel image rotlet. The no-slip condition on  $z = 0$ ,  $\varrho > 1$ , requires that

$$v_1(\varrho, 0) = 0, \quad \varrho > 1, \tag{2.5}$$

and following Keer [5], (2.5) is satisfied identically by representing  $v_1$  in the form

$$v_1(\varrho, z) = - \int_0^1 t^{3/2} j_1(t) \left\{ \int_0^\infty \alpha^{1/2} J_{3/2}(\alpha t) J_1(\alpha \varrho) e^{-\alpha z} d\alpha \right\} dt, \quad z \geq 0, \tag{2.6}$$

where the continuous function  $j_1(t)$  is to be determined. In the pore region II separation of variables in (2.3) provides the form

$$v^{II}(\varrho, z) = \sum_{n=1}^\infty (A_n e^{\sigma_n z} + B_n e^{-\sigma_n(z+2l)}) J_1(\sigma_n \varrho), \quad -2l \leq z \leq 0, \tag{2.7}$$

where, in order to satisfy the no-slip condition on the pore wall  $\varrho = 1$ , the  $\sigma_n$  are the positive zeros in ascending order of magnitude of the Bessel function  $J_1(x)$ , and the  $A_n$ ,  $B_n$  are constants. Finally in the singularity-free region III, a velocity field satisfying the no-slip condition on the membrane wall  $z = -2l$ ,  $\varrho > 1$ , is again supplied by the Keer form

$$v^{III}(\varrho, z) = \int_0^1 t^{3/2} j_3(t) \left\{ \int_0^\infty \alpha^{1/2} J_{3/2}(\alpha t) J_1(\alpha \varrho) e^{\alpha(z+2l)} d\alpha \right\} dt, \quad z \leq -2l. \tag{2.8}$$

The unknown functions  $j_1(t)$ ,  $j_3(t)$  and the sequences of coefficients  $\{A_n\}$ ,  $\{B_n\}$  in (2.6) through (2.8) are now found, using the methods developed in [1], by requiring the continuity

of velocity and shear stress across the pore/half-space interfaces at  $z = 0$  and  $z = -2l$ . Explicitly we have the conditions

$$v^I(\varrho, 0) = v^{II}(\varrho, 0), \tag{2.9}$$

$$v^{II}(\varrho, -2l) = v^{III}(\varrho, -2l), \tag{2.10}$$

$$\frac{\partial v^I}{\partial z}(\varrho, 0) = \frac{\partial v^{II}}{\partial z}(\varrho, 0), \tag{2.11}$$

$$\frac{\partial v^{II}}{\partial z}(\varrho, -2l) = \frac{\partial v^{III}}{\partial z}(\varrho, -2l), \tag{2.12}$$

all for  $0 \leq \varrho \leq 1$ , which reduce, using results given in [5], to

$$-\left(\frac{2}{\pi}\right)^{1/2} \varrho \int_{\varrho}^1 \frac{j_1(t)}{(t^2 - \varrho^2)^{1/2}} dt = \sum_{n=1}^{\infty} (A_n + B_n e^{-2\sigma_n l}) J_1(\sigma_n \varrho), \tag{2.13}$$

$$-\left(\frac{2}{\pi}\right)^{1/2} \varrho \int_{\varrho}^1 \frac{j_3(t)}{(t^2 - \varrho^2)^{1/2}} dt = \sum_{n=1}^{\infty} (A_n e^{-2\sigma_n l} + B_n) J_1(\sigma_n \varrho), \tag{2.14}$$

$$-\frac{6h\varrho}{(\varrho^2 + h^2)^{5/2}} + \left(\frac{2}{\pi}\right)^{1/2} \frac{1}{\varrho^2} \frac{d}{d\varrho} \int_{\varrho}^1 \frac{t^3 j_1(t)}{(\varrho^2 - t^2)^{1/2}} dt = \sum_{n=1}^{\infty} \sigma_n (A_n - B_n e^{-2\sigma_n l}) J_1(\sigma_n \varrho), \tag{2.15}$$

and

$$\left(\frac{2}{\pi}\right)^{1/2} \frac{1}{\varrho^2} \int_{\varrho}^1 \frac{t^3 j_3(t)}{(\varrho^2 - t^2)^{1/2}} dt = \sum_{n=1}^{\infty} \sigma_n (A_n e^{-2\sigma_n l} - B_n) J_1(\sigma_n \varrho), \quad 0 \leq \varrho \leq 1. \tag{2.16}$$

The integral equations (2.15) and (2.16) can now be solved to express  $j_1(t)$  and  $j_3(t)$  in terms of the coefficients  $\{A_n\}$ ,  $\{B_n\}$ , with the results

$$j_1(t) = t^{-1/2} \sum_{n=1}^{\infty} \sigma_n^{1/2} (A_n - B_n e^{-2\sigma_n l}) J_{3/2}(\sigma_n t) + \left(\frac{2}{\pi}\right)^{1/2} \frac{4t}{(t^2 + h^2)^2}, \tag{2.17}$$

and

$$j_3(t) = t^{-1/2} \sum_{n=1}^{\infty} \sigma_n^{1/2} (A_n e^{-2\sigma_n l} - B_n) J_{3/2}(\sigma_n t), \quad 0 \leq t \leq 1. \tag{2.18}$$

Turning next to (2.13) and (2.14) we multiply both by  $\varrho J_1(\sigma_n \varrho)$  and integrate from  $\varrho = 0$  to  $\varrho = 1$ . After some manipulation we find

$$-\sigma_m^{-1/2} \int_0^1 t^{3/2} J_{3/2}(\sigma_m t) j_1(t) dt = \frac{1}{2} (A_m + B_m e^{-2\sigma_m l}) J_0^2(\sigma_m), \tag{2.19}$$

and

$$\sigma_m^{-1/2} \int_0^1 t^{3/2} J_{3/2}(\sigma_m t) j_3(t) dt = \frac{1}{2}(A_m e^{-2\sigma_m l} + B_m) J_0^2(\sigma_m). \tag{2.20}$$

Infinite sets of linear equations for the  $\{A_n\}$ ,  $\{B_n\}$  now follow by eliminating  $j_1(t)$  and  $j_3(t)$  between (2.17), (2.18), (2.19) and (2.20), viz.

$$\begin{aligned} & \frac{1}{2} \pi \sigma_m J_0^2(\sigma_m) (A_m + B_m e^{-2\sigma_m l}) \\ & + \sum_{n=1}^{\infty} (A_n - B_n e^{-2\sigma_n l}) \left( \frac{\sin(\sigma_n - \sigma_m)}{\sigma_n - \sigma_m} + \frac{\sin(\sigma_n + \sigma_m)}{\sigma_n + \sigma_m} - \frac{2 \sin \sigma_m \sin \sigma_n}{\sigma_m \sigma_n} \right) \\ & = - \frac{4}{1 + h^2} \frac{\sin \sigma_m}{\sigma_m} + 4 \int_0^1 \frac{h^2 - t^2}{(t^2 + h^2)^2} \cos \sigma_m t, \end{aligned} \tag{2.21}$$

and

$$\begin{aligned} & \frac{1}{2} \pi \sigma_m J_0^2(\sigma_m) (A_m e^{-2\sigma_m l} + B_m) \\ & - \sum_{n=1}^{\infty} (A_n e^{-2\sigma_n l} - B_n) \left( \frac{\sin(\sigma_n - \sigma_m)}{\sigma_n - \sigma_m} + \frac{\sin(\sigma_n + \sigma_m)}{\sigma_n + \sigma_m} - \frac{2 \sin \sigma_m \sin \sigma_n}{\sigma_m \sigma_n} \right) = 0, \\ & m = 1, 2, \dots \end{aligned} \tag{2.22}$$

In (2.21), (2.22) and elsewhere a factor  $(\sigma_m - \sigma_n)^{-1} \sin(\sigma_m - \sigma_n)$  is interpreted as unity when  $m = n$ .

The systems of equations (2.21) and (2.22) are solved by truncation to finite sets, and  $j_1(t)$ ,  $j_3(t)$  then follow from (2.17), (2.18). In the limit  $l \rightarrow \infty$ , (2.22) becomes a set of homogeneous equations with solution  $B_n \equiv 0$ ,  $n = 1, 2, \dots$ . The set (2.21) then reduces to that derived in [1] for a semi-infinite pore.

When the rotlet is placed within the pore at  $z = -h$ ,  $0 < h < 2l$ , the representations (2.4) and (2.7) must be modified. Appropriate forms are

$$v^I(\varrho, z) = v_1(\varrho, z), \quad z > 0, \tag{2.23}$$

where  $v_1$  is given by (2.6), and

$$\begin{aligned} v^{II}(\varrho, z) &= \frac{\varrho}{R_2^3} - \frac{2}{\pi} \int_0^{\infty} \frac{k K_1(k)}{I_1(k)} I_1(k\varrho) \cos k(z + h) dk \\ &+ \sum_{n=1}^{\infty} (A_n e^{\sigma_n z} + B_n e^{\sigma_n(z+2l)}) J_1(\sigma_n \varrho), \quad -2l \leq z \leq 0. \end{aligned} \tag{2.24}$$

In (2.24) the first two terms constitute the velocity field produced by a rotlet placed on the axis of an infinitely long cylinder [6], and (2.24) satisfies identically the no-slip condition on

the pore walls. Proceeding as in the previous paragraph the simultaneous sets of equations for the  $\{A_n\}$ ,  $\{B_n\}$  are again found to have the forms (2.21) and (2.22) but with their right-hand sides replaced by

$$\pi\sigma_m(\gamma_0(m, h) + e^{-\sigma_m h}) \quad \text{and} \quad \pi\sigma_m(\gamma_0(m, h - 2l) + e^{-\sigma_m(z-2l)})$$

respectively, where

$$\begin{aligned} \gamma_0(m, h) &= \frac{4}{\pi^2 \sigma_m^2} \int_0^\infty \frac{K_1(k)}{I_1(k)} \\ &\times \left\{ \sin \sigma_m \sinh k - \frac{k\sigma_m^2 \sin \sigma_m \cosh k + k^2 \sigma_m \cos \sigma_m \sinh k}{k^2 + \sigma_m^2} \right\} \sin kh \, dk \\ &+ \frac{2 \sin \sigma_m}{\pi \sigma_m^2 (1 + h^2)} - \frac{2}{\pi \sigma_m} \int_0^1 \frac{h^2 - t^2}{(t^2 + h^2)^2} \cos \sigma_m t \, dt. \end{aligned} \tag{2.25}$$

The importance of the rotlet solution lies in the fact that it can be used to determine the effect of the membrane on the torque  $T$  required to maintain the steady rotation of an axisymmetric particle, the axis of rotation being the pore axis. Let  $T_\infty$  be the corresponding torque for the rotation of the body with angular speed  $\Omega$  in an unbounded fluid. Then referring to [1] and [2], the ratio  $T_\infty/T$  is given by

$$\frac{T_\infty}{T} = 1 - \frac{T_\infty}{8\pi\mu\Omega c^3} C_1 + O\left(\frac{a}{L}\right)^5, \tag{2.26}$$

where  $c$  is the pore radius in physical variables,  $b = c|h|$ , and  $L = \max(b, c)$ . Also the torque factor  $C_1$  is defined by

$$C_1 = -\frac{1}{2} \lim_{\substack{\varrho \rightarrow 0 \\ z \rightarrow \pm h}} \frac{1}{\varrho} \frac{\partial}{\partial \varrho} (\varrho v^*), \tag{2.27}$$

where  $v^*$  is the regular part (as  $\varrho \rightarrow 0$ ,  $z \rightarrow h$ ) of (2.4) for the particle situated in  $z > 0$  and of (2.24) (as  $\varrho \rightarrow 0$ ,  $z \rightarrow -h$ ) for the particle within the pore. Direct evaluation of (2.27) shows that for the particle in the half-space

$$\begin{aligned} C_1 &= -\frac{1}{8h^3} + \frac{(h^2 + 3)(1 - 3h^2)}{6\pi(h^2 + 1)^3} + \frac{1}{2\pi h^3} \tan^{-1}(1/h) + \frac{1}{\pi} \sum_{n=1}^\infty (A_n - B_n e^{-2\sigma_n l}) \\ &\times \left\{ -\frac{\sin \sigma_n}{\sigma_n(h^2 + 1)^2} + \int_0^1 \frac{h^2 - t^2}{(h^2 + t^2)^2} \cos \sigma_n t \, dt \right\}, \end{aligned} \tag{2.28}$$

whereas for the particle at  $z = -h$ ,  $0 < h < 2l$ , inside the pore,

$$C_1 = -\frac{1}{\pi} \int_0^\infty \frac{k^2 K_1(k)}{I_1(k)} \, dk - \frac{1}{2} \sum_{n=1}^\infty \sigma_n \{A_n e^{-\sigma_n h} + B_n e^{-\sigma_n(2l-h)}\}, \tag{2.29}$$

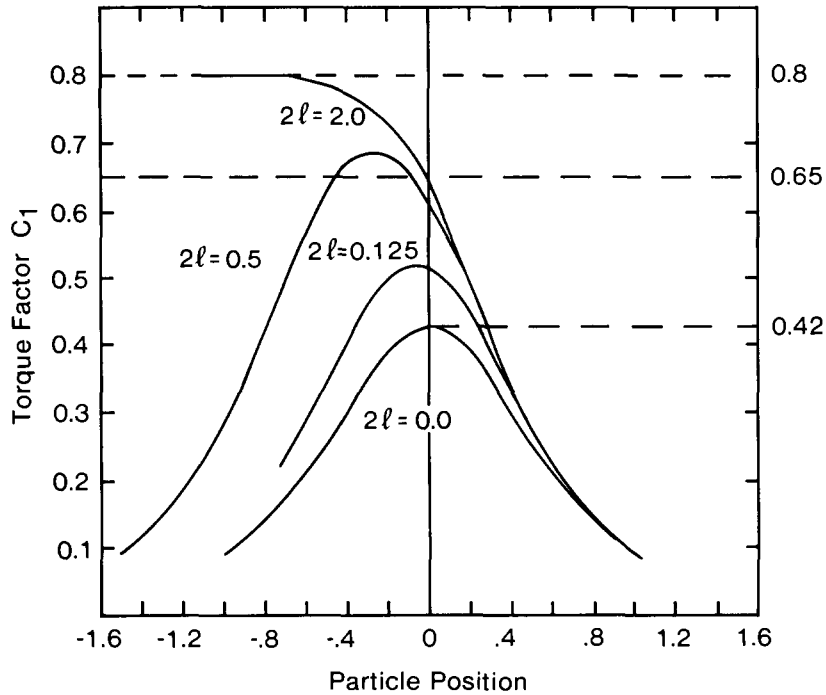


Fig. 2. The torque factor  $C_1$  plotted against particle position for various pore lengths.

The computation of  $C_1$  is affected by first truncating the infinite sets of equations (2.21) and (2.22) (or their modified forms for the rotlet inside the pore) to the same upper limit  $N$  and using an appropriate numerical linear-equation solving routine. Numerical difficulties in solving the resulting equations were experienced when the physical parameters  $h, l$  were small, and an inspection of the condition number of the coefficient matrix disclosed ill-conditioning. Use of the standard NAG routines produced some wildly inaccurate solutions, but application of the method of conjugate gradients [7] provided much improved and acceptable results. Figure 2 shows values of the torque factor for various rotlet positions and pore lengths. For  $h > 0.1$ ,  $N$  was taken to be 90, whereas for  $0 < h < 0.1$  it was necessary to use values of  $N$  up to 500 in order to secure convergence of (2.28) and (2.29). Figure 2 shows that for the rotlet outside the pore with a membrane thickness of about one pore radius, the torque correction is indistinguishable from that for a rotlet outside a semi-infinite pore.

The limiting value of  $C_1$  when  $h = 0$  requires special attention. From (2.29) with  $h = 0$  we have

$$C_1 = -\frac{1}{\pi} \int_0^\infty \frac{k^2 K_1(k)}{I_1(k)} dk - \frac{1}{2} \sum_{n=1}^\infty \sigma_n (A_n + B_n e^{-2\sigma_n l}). \quad (2.30)$$

Observing the slow-convergence behaviour of the partial sums of the infinite series in (2.30) it became very evident that direct summation would be impossible. However, applying a Shanks transform [8] it proved possible to consider all pore lengths. In the limit of a zero-length pore, the value 0.42 was obtained for  $C_1$ , in exact agreement with Davis et al.

[3], whereas for infinite  $l$ , the interpolation value 0.65 of [1] was reproduced. Thus it appears that a combination of large truncation values for  $N$  ( $\sim 500$ ), the conjugate gradient method and a non-linear convergence accelerator of Shanks overcomes the difficulties in the case  $h = 0$  first noted in [1].

### 3. The Stokeslet problem

In order to model a particle translating along the pore axis we next consider the problem in which the rotlet singularity of section 2 is replaced by a Stokeslet of unit strength, oriented parallel to the pore axis. We also suppose that a difference in pressures at infinity in the half-space chambers  $z > 0$  and  $z < -2l$  drives a volumetric flow with flux  $M$  through the pore. As in the rotlet configuration it is convenient to consider the cases with the singularity at  $z = h$  ( $> 0$ ) and  $z = -h$  separately, beginning with the  $z = h$  case, i.e., the singularity outside the pore.

Observe that the velocity fields in the three flow regions have both radial and transverse components; these fields must be found so as to satisfy the no-slip conditions on the membrane/pore surfaces and also to ensure continuity of velocity and stress across the pore/half-space interfaces. Thus it is essential to optimize the velocity representations used and we employ those developed in [1], with appropriate modifications to allow for the finite pore length and the existence of region III. Thus, in  $z > 0$  we write the velocity and pressure fields as

$$\mathbf{v}^I = \mathbf{v}_0 + z\nabla\phi_1 - \phi_1\mathbf{z} + z\nabla\psi_1 - \psi_1\mathbf{z} + \nabla\tilde{\omega}_1, \quad (3.1)$$

$$p^I = p_0 + 2\mu \left( \frac{\partial\phi_1}{\partial z} + \frac{\partial\psi_1}{\partial z} \right), \quad (3.2)$$

where  $\phi_1$ ,  $\psi_1$ ,  $\tilde{\omega}_1$  are axisymmetric harmonic functions of  $(\varrho, z)$  with  $\psi_1 = \partial\tilde{\omega}_1/\partial z$ , and  $(\mathbf{v}_0, p_0)$  are the velocity and pressure fields given in [1] for the problem of an axial Stokeslet of unit strength situated at  $z = h$  in front of a rigid plane wall occupying  $z = 0$ . Explicitly,

$$\begin{aligned} \mathbf{v}_0 = & \left[ \varrho(z-h) \left( \frac{1}{R_1^3} - \frac{1}{R_2^3} \right) - \frac{6h\varrho z(z+h)}{R_2^5} \right] \mathbf{e} \\ & + \left[ 2 \left( \frac{1}{R_1} - \frac{1}{R_2} \right) - \varrho^2 \left( \frac{1}{R_1^3} - \frac{1}{R_2^3} \right) + \frac{2hz}{R_2^5} [\varrho^2 - 2(z+h)^2] \right] \mathbf{z}, \end{aligned} \quad (3.3)$$

$$p_0 = p_\infty + \frac{2\mu(z-h)}{R_1^3} + 2\mu \left( \frac{h-z}{R_2^3} - \frac{6h(z+h)^2}{R_2^5} \right), \quad (3.4)$$

where  $p_\infty$  is the pressure as  $z \rightarrow \infty$ . The  $\phi_1$ -dependent part of (3.1) has zero  $\varrho$ -component on  $z = 0$ , whereas the terms in  $\psi_1$ ,  $\tilde{\omega}_1$  provide a velocity field with zero  $z$ -component on  $z = 0$ . In a similar manner the velocity and pressure fields in the fluid region III ( $z < -2l$ )



are represented in terms of harmonic functions  $\phi_3, \psi_3$  and  $\tilde{\omega}_3$  as

$$\mathbf{v}^{\text{III}} = (z + 2l)\nabla\phi_3 - \phi_3\mathbf{z} + (z + 2l)\nabla\psi_3 - \psi_3\mathbf{z} + \nabla\tilde{\omega}_3, \tag{3.5}$$

$$p^{\text{III}} = p_{-\infty} + 2\mu\left(\frac{\partial\phi_3}{\partial z} + \frac{\partial\psi_3}{\partial z}\right), \tag{3.6}$$

where  $\psi_3 = \partial\tilde{\omega}_3/\partial z$  and  $p_{-\infty}$  is the pressure as  $z \rightarrow -\infty$ .

We now take integral representations of  $\phi_k, \tilde{\omega}_k$  ( $k = 1, 3$ ) so as to satisfy the no-slip conditions on  $z = 0, \varrho > 1$  and  $z = -2l, \varrho > 1$ . Following Keer [5] we write

$$\phi_k(\varrho, z) = \mp \int_0^1 j_k(t) \left\{ \int_0^\infty \sin \alpha t J_0(\alpha\varrho) e^{\mp\alpha\{z+(k-1)l\}} d\alpha \right\} dt \tag{3.7}$$

for  $k = 1, 3^*$ , and since  $\cos \theta \partial\tilde{\omega}_k/\partial\varrho$  is harmonic we have as in Section 2 the appropriate forms

$$\frac{\partial\tilde{\omega}_k}{\partial\varrho}(\varrho, z) = \mp \int_0^1 t^{3/2} g_k(t) \left\{ \int_0^\infty \alpha^{1/2} J_{3/2}(\alpha t) J_1(\alpha\varrho) e^{\mp\alpha\{z+(k-1)l\}} d\alpha \right\} dt. \tag{3.8}$$

In (3.7) and (3.8) the upper signs pertain to  $k = 1$  and the lower to  $k = 3$ . The forms (3.7) and (3.8) imply that  $\phi_k$  and  $\partial\tilde{\omega}_k/\partial\varrho$  are zero on  $z = 0$  ( $k = 1$ ) and  $z = -2l$  ( $k = 3$ ) for  $\varrho > 1$  thereby securing the vanishing of  $\mathbf{v}^{\text{I}}$  and  $\mathbf{v}^{\text{III}}$  on the relevant membrane faces. Since the flux through both  $z = 0$  and  $z = -2l, 0 \leq \varrho \leq 1$ , is  $M$  we also have from (3.1), (3.5) and (3.7) the relations

$$\int_0^1 t j_1(t) dt = - \int_0^1 t j_3(t) dt = \frac{M}{2\pi}. \tag{3.9}$$

In the pore region  $-2l \leq z \leq 0, 0 \leq \varrho \leq 1$ , modified forms of the velocity and pressure fields of [1] are employed, namely

$$\mathbf{v}^{\text{II}} = (E_0\varrho^2 + F_0)\mathbf{z} + z\nabla U - U\mathbf{z} + z\nabla V - V\mathbf{z} + \nabla W + \varrho\boldsymbol{\theta} \times \nabla X - 2X\mathbf{z} + \nabla Y, \tag{3.10}$$

$$p^{\text{II}} = P + 2\mu \left\{ 2E_0z + \frac{\partial U}{\partial z} + \frac{\partial V}{\partial z} + \frac{\partial X}{\partial z} \right\}, \tag{3.11}$$

where  $E_0, F_0$  are constants,  $P$  is a constant reference pressure, and  $U, V, W, X, Y$  are axially symmetric harmonic functions with  $V = \partial W/\partial z$ . These harmonics are expanded

\* Evaluation of the infinite integral in (3.7) produces the Green-Zerna [9] contour-integral representation used in [1].

as

$$\begin{aligned}
 U &= \sum_{n=1}^{\infty} (A_n e^{\sigma_n z} + B_n e^{-\sigma_n(z+2l)}) J_0(\sigma_n \varrho), \\
 V &= \sum_{n=1}^{\infty} (C_n e^{\sigma_n z} + D_n e^{-\sigma_n(z+2l)}) J_0(\sigma_n \varrho), \\
 W &= \sum_{n=1}^{\infty} \sigma_n^{-1} (C_n e^{\sigma_n z} - D_n e^{-\sigma_n(z+2l)}) J_0(\sigma_n \varrho), \\
 X &= \sum_{n=1}^{\infty} (E_n \cos \alpha_n z + F_n \sin \alpha_n z) I_0(\sigma_n \varrho), \\
 Y &= \sum_{n=1}^{\infty} (G_n \cos \alpha_n z + H_n \sin \alpha_n z) I_0(\sigma_n \varrho), \tag{3.12}
 \end{aligned}$$

where  $\alpha_n = n\pi/l$  and  $A_n$  through  $H_n$  are constants. Note that the contribution to  $\mathbf{v}^{\text{II}}$  which would arise from the missing constant terms ( $n = 0$ ) in the Fourier expansions (3.12)<sub>4</sub> and (3.12)<sub>5</sub>, is subsumed in the term  $(E_0 + F_0 \varrho^2)\mathbf{z}$ ; further, the condition that the flux through the pore be  $M$  gives the relation

$$\frac{1}{2}E_0 + F_0 = \frac{M}{\pi}. \tag{3.13}$$

Consider next the no-slip conditions on the pore walls, namely

$$\mathbf{v}^{\text{II}} \cdot \boldsymbol{\varrho} = \mathbf{v}^{\text{II}} \cdot \mathbf{z} = 0 \quad \text{on} \quad \varrho = 1, \quad -2l \leq z \leq 0. \tag{3.14}$$

Use of (3.10) and (3.12) in (3.14), followed by applications of the Fourier inversion theorem with respect to  $z$  then yield sets of linear equations from which the coefficients  $E_m$ ,  $F_m$ ,  $G_m$  and  $H_m$ ,  $m \geq 1$ , can be expressed as linear functions of  $A_n$  through  $D_n$ . Explicitly, for  $m = 1, 2, \dots$ ,

$$E_m = \frac{I_1(\alpha_m)H_m}{I_0(\alpha_m)} = \frac{I_1(\alpha_m)}{l\alpha_m\Delta(\alpha_m)} \sum_{n=1}^{\infty} \Psi_0(n, m) J_0(\sigma_n), \tag{3.15}$$

$$F_m = -\frac{I_1(\alpha_m)G_m}{I_0(\alpha_m)} = \frac{I_1(\alpha_m)}{l\alpha_m\Delta(\alpha_m)} \sum_{n=1}^{\infty} \Psi_1(n, m) J_0(\sigma_n), \tag{3.16}$$

where

$$\Delta(\alpha_m) = I_1^2(\alpha_m) - I_0(\alpha_m)I_2(\alpha_m) \tag{3.17}$$

and  $\Psi_0, \Psi_1$  are linear functions of  $A_n, \dots, D_n$  defined by

$$\begin{aligned} \Psi_0(n, m) = & -\frac{\sigma_n}{(\sigma_n^2 + \alpha_m^2)^2} [(1 - e^{-2\sigma_n l})\{(2A_n + 2B_n + C_n + D_n)\sigma_n^2 - (C_n + D_n)\alpha_m^2\} \\ & - 2\sigma_n l(\sigma_n^2 + \alpha_m^2)\{(A_n + C_n)e^{-2\sigma_n l} + B_n + D_n\}], \end{aligned} \quad (3.18)$$

$$\begin{aligned} \Psi_1(n, m) = & \frac{\alpha_m}{(\sigma_n^2 + \alpha_m^2)^2} [(1 - e^{-2\sigma_n l})\{(3\sigma_n^2 + \alpha_m^2)(A_n - B_n) + 2\sigma_n^2(C_n - D_n)\} \\ & - 2\sigma_n l(\sigma_n^2 + \alpha_m^2)\{(A_n + C_n)e^{-2\sigma_n l} - B_n - D_n\}]. \end{aligned} \quad (3.19)$$

Further the  $m = 0$  Fourier contribution provides the equation

$$\begin{aligned} 2l(E_0 + F_0) = & \sum_{n=1}^{\infty} \sigma_n^{-1} [(1 - e^{-2\sigma_n l})(2A_n + 2B_n + C_n + D_n) \\ & - 2\sigma_n l\{(A_n + C_n)e^{-2\sigma_n l} + B_n + D_n\}]J_0(\sigma_n). \end{aligned} \quad (3.20)$$

Thus, using (3.13) and (3.20),  $E_0$  and  $F_0$  can be found in terms of  $M$  and the coefficients  $\{A_n, \dots, D_n\}$ ; in particular

$$\begin{aligned} E_0 = & -\frac{2M}{\pi} + \frac{1}{l} \sum_{n=1}^{\infty} \sigma_n^{-1} [(2A_n + 2B_n + C_n + D_n)(1 - e^{-2\sigma_n l}) \\ & - 2\sigma_n l\{(A_n + C_n)e^{-2\sigma_n l} + B_n + D_n\}]J_0(\sigma_n). \end{aligned} \quad (3.21)$$

The velocity and pressure fields in the three fluid regions now comply with the kinematic no-slip conditions, and it remains to derive equations for computing the functions  $j_k(t), g_k(t)$ ,  $k = 1, 3$  and the four coefficient sequences  $\{A_n\}$  through  $\{D_n\}$ , all in terms of the prescribed flux  $M$ . A further eight conditions are to be satisfied, namely the continuity of  $\mathbf{v} \cdot \boldsymbol{\rho}$ ,  $\mathbf{v} \cdot \mathbf{z}$ , the normal and the shear stress components at the interfaces  $z = 0$  and  $z = -2l$ ,  $0 \leq \varrho \leq 1$ , and these, together with (3.20) and the flux conditions (3.9), (3.13) make the problem fully determinate although algebraically very complicated. In what follows much of this algebraic complexity is omitted whilst preserving the essential steps of the argument.

Consider first the continuity of  $\mathbf{v} \cdot \boldsymbol{\rho}$  across  $z = 0$  and  $z = -2l$ ,  $0 \leq \varrho \leq 1$ ; from the representations (3.1), (3.5) and (3.10) two equations analogous to (2.13) and (2.14) result, namely

$$\begin{aligned} \left(\frac{2}{\pi}\right)^{1/2} \varrho \int_{\varrho}^1 \frac{g_1(t)}{(t^2 - \varrho^2)^{1/2}} dt = & \sum_{n=1}^{\infty} (C_n - D_n e^{-2\sigma_n l})J_1(\sigma_n \varrho) \\ & - \sum_{n=1}^{\infty} \alpha_n \{\varrho I_0(\alpha_n \varrho)F_n + I_1(\alpha_n \varrho)G_n\}, \end{aligned} \quad (3.22)$$

and

$$\begin{aligned} & \left(\frac{2}{\pi}\right)^{1/2} \varrho \int_{\varrho}^1 \frac{g_3(t)}{(t^2 - \varrho^2)^{1/2}} dt \\ &= \sum_{n=1}^{\infty} \{2\sigma_n l(A_n e^{-2\sigma_n l} + B_n) + (2\sigma_n l - 1)e^{-2\sigma_n l} + (2\sigma_n l + 1)D_n\} J_1(\sigma_n \varrho) \\ &+ \sum_{n=1}^{\infty} \alpha_n \{\varrho I_0(\alpha_n \varrho) F_n + I_1(\alpha_n \varrho) G_n\}, \quad 0 \leq \varrho \leq 1. \end{aligned} \tag{3.23}$$

Similarly, the continuity of  $\mathbf{v} \cdot \mathbf{z}$  at  $z = 0$  and  $z = -2l$  supplies the equations

$$\begin{aligned} \int_{\varrho}^1 \frac{j_1(t)}{(t^2 - \varrho^2)^{1/2}} dt &= E_0 \varrho^2 + F_0 - \sum_{n=1}^{\infty} (A_n + B_n e^{-2\sigma_n l}) J_0(\sigma_n \varrho) \\ &- \sum_{n=1}^{\infty} [\{\alpha_n \varrho I_1(\alpha_n \varrho) + 2I_0(\alpha_n \varrho)\} E_n - \alpha_n I_0(\alpha_n \varrho) H_n], \end{aligned} \tag{3.24}$$

and

$$\begin{aligned} - \int_{\varrho}^1 \frac{j_3(t)}{(t^2 - \varrho^2)^{1/2}} dt &= E_0 \varrho^2 + F_0 \\ &- \sum_{n=1}^{\infty} \{(2\sigma_n l + 1)e^{-2\sigma_n l} A_n - (2\sigma_n l - 1)B_n + 2\sigma_n l(C_n e^{-2\sigma_n l} - D_n)\} J_0(\sigma_n \varrho) \\ &- \sum_{n=1}^{\infty} [\{\alpha_n \varrho I_1(\alpha_n \varrho) + 2I_0(\alpha_n \varrho)\} E_n - \alpha_n I_0(\alpha_n \varrho) H_n], \quad 0 \leq \varrho \leq 1, \end{aligned} \tag{3.25}$$

and  $E_n, \dots, H_n$  in (3.22) through (3.25) can be eliminated in favour of  $A_n, \dots, D_n$  using (3.15) and (3.16).

Recalling that  $J_1(\sigma_n) = 0, n = 1, 2, \dots$ , the Fourier-Bessel inversion theorem can be applied to (3.22) and (3.23) to show that for  $m = 1, 2, \dots$

$$\begin{aligned} & \frac{1}{2} \sigma_m J_0^2(\sigma_m)(C_m - D_m e^{-2\sigma_m l}) \\ &= \left(\frac{2}{\pi}\right)^{1/2} \int_0^1 \left(\frac{\sin \sigma_m t}{\sigma_m} - t \cos \sigma_m t\right) g_1(t) dt + 2\sigma_m^2 J_0(\sigma_m) \sum_{n=1}^{\infty} \frac{\alpha_n^2 I_1(\alpha_n)}{(\sigma_m^2 + \alpha_n^2)^2} F_n \end{aligned} \tag{3.26}$$

and

$$\begin{aligned} & \frac{1}{2} \sigma_m J_0^2(\sigma_m) \{2\sigma_m l(A_m e^{-2\sigma_m l} + B_m) + (2\sigma_m l - 1)e^{-2\sigma_m l} + (2\sigma_m l + 1)D_m\} \\ &= \left(\frac{2}{\pi}\right)^{1/2} \int_0^1 \left(\frac{\sin \sigma_m t}{\sigma_m} - t \cos \sigma_m t\right) g_3(t) dt - 2\sigma_m^2 J_0(\sigma_m) \sum_{n=1}^{\infty} \frac{\alpha_n^2 I_1(\alpha_n)}{(\sigma_m^2 + \alpha_n^2)^2} F_n. \end{aligned} \tag{3.27}$$

In a similar manner since  $J_1(\sigma_n) = -J'_0(\sigma_n) = 0$ , the Fourier–Dini inversion theorem in the “ $H + v = 0$ ” case [10, p. 144] applied to (3.24) and (3.25) yields, for  $m = 1, 2, \dots$ ,

$$\begin{aligned} \frac{1}{2}\sigma_m J_0^2(\sigma_m)(A_m + B_m e^{-2\sigma_m l}) &= 2\sigma_m^{-1} J_0(\sigma_m) E_0 \\ &- \int_0^1 j_1(t) \sin \sigma_m t \, dt - 2J_0(\sigma_m) \sigma_m^3 \sum_{n=1}^{\infty} \frac{\alpha_n I_1(\alpha_n)}{(\sigma_m^2 + \alpha_n^2)^2} E_n, \end{aligned} \quad (3.28)$$

and

$$\begin{aligned} \frac{1}{2}\sigma_m J_0^2(\sigma_m) \{ (2\sigma_m l + 1)e^{-2\sigma_m l} A_m - (2\sigma_m l - 1)B_m + 2\sigma_m l (C_m e^{-2\sigma_m l} - D_m) \} \\ = 2\sigma_m^{-1} J_0(\sigma_m) E_0 + \int_0^1 j_3(t) \sin \sigma_m t \, dt \\ - 2J_0(\sigma_m) \sigma_m^3 \sum_{n=1}^{\infty} \frac{\alpha_n I_1(\alpha_n)}{(\sigma_m^2 + \alpha_n^2)^2} E_n. \end{aligned} \quad (3.29)$$

Finally the stress continuity conditions on  $z = 0$  and  $z = -2l$ ,  $0 \leq \varrho \leq 1$ , are imposed. Using the expressions for the stress components  $\tau_{\varrho z}$  and  $\tau_{zz}$  detailed in [1], we find the following relations analogous to (2.15) and (2.16):

$$\begin{aligned} \left(\frac{2}{\pi}\right)^{1/2} \frac{1}{\varrho^2} \frac{d}{d\varrho} \int_0^{\varrho} \frac{t^3 g_1(t)}{(\varrho^2 - t^2)^{1/2}} dt &= \frac{6h^2 \varrho}{(\varrho^2 + h^2)^{5/2}} + E_0 \varrho - \sum_{n=1}^{\infty} \sigma_n (C_n + D_n e^{-2\sigma_n l}) J_0(\sigma_n \varrho) \\ &- \sum_{n=1}^{\infty} \alpha_n [\{\alpha_n \varrho I_0(\alpha_n \varrho) + I_1(\alpha_n \varrho)\} E_n - \alpha_n I_1(\alpha_n \varrho) H_n], \end{aligned} \quad (3.30)$$

$$\begin{aligned} \left(\frac{2}{\pi}\right)^{1/2} \frac{1}{\varrho^2} \frac{d}{d\varrho} \int_0^{\varrho} \frac{t^3 g_3(t)}{(\varrho^2 - t^2)^{1/2}} dt &= E_0 \varrho \\ &+ \sum_{n=1}^{\infty} \sigma_n [2\sigma_n l (A_n e^{-2\sigma_n l} - B_n) + \{(2\sigma_n l - 1)e^{-2\sigma_n l} C_n - (2\sigma_n l + 1)D_n\}] J_1(\sigma_n \varrho) \\ &- \sum_{n=1}^{\infty} \alpha_n [\{\alpha_n \varrho I_0(\alpha_n \varrho) + I_1(\alpha_n \varrho)\} E_n - \alpha_n I_1(\alpha_n \varrho) H_n], \end{aligned} \quad (3.31)$$

$$\begin{aligned} \frac{1}{\varrho} \frac{d}{d\varrho} \int_0^{\varrho} \frac{t j_1(t)}{(\varrho^2 - t^2)^{1/2}} dt &= Q_1 + \frac{6h^3}{(\varrho^2 + h^2)^{5/2}} + \sum_{n=1}^{\infty} \sigma_n (A_n - B_n e^{-2\sigma_n l}) J_0(\sigma_n \varrho) \\ &+ \sum_{n=1}^{\infty} \alpha_n [\{3I_0(\alpha_n \varrho) + \alpha_n \varrho I_1(\alpha_n \varrho)\} F_n + \alpha_n I_0(\alpha_n \varrho) G_n], \end{aligned} \quad (3.32)$$

and

$$\begin{aligned} \frac{1}{\varrho} \frac{d}{d\varrho} \int_0^{\varrho} \frac{t j_3(t)}{(\varrho^2 - t^2)^{1/2}} dt &= Q_2 - 4E_0 l \\ &+ \sum_{n=1}^{\infty} \sigma_n \{ (2\sigma_n l + 1) e^{-2\sigma_n l} A_n + (2\sigma_n l - 1) B_n + 2\sigma_n l (C_n e^{-2\sigma_n l} + D_n) \} J_0(\sigma_n \varrho) \\ &+ \sum_{n=1}^{\infty} \alpha_n \{ [3I_0(\alpha_n \varrho) + \alpha_n \varrho I_1(\alpha_n \varrho)] F_n + \alpha_n I_0(\alpha_n \varrho) G_n \}, \end{aligned} \quad (3.33)$$

all for  $0 \leq \varrho \leq 1$ , where  $Q_1 = (P - p_{\infty})/2\mu$ ,  $Q_2 = (P - p_{-\infty})/2\mu$ . Proceeding as in Section 2, integral equations (3.30) through (3.33) are now solved for  $j_1(t)$ ,  $j_3(t)$ ,  $g_1(t)$  and  $g_3(t)$  with the results that for  $0 \leq t \leq 1$ ,

$$j_1(t) = \frac{2tQ_1}{\pi} + \frac{4t(t^2 + 3h^2)}{\pi(t^2 + h^2)^2} + \frac{2}{\pi} \sum_{n=1}^{\infty} (A_n - B_n e^{-2\sigma_n l}) \sin \sigma_n t + \frac{2}{\pi} \sum_{n=1}^{\infty} G(\alpha_n, t) F_n, \quad (3.34)$$

$$\begin{aligned} j_3(t) &= \frac{2t(Q_2 - 4E_0 l)}{\pi} + \frac{2}{\pi} \sum_{n=1}^{\infty} \{ (2\sigma_n l + 1) e^{-2\sigma_n l} A_n + (2\sigma_n l - 1) B_n \\ &+ 2\sigma_n l (C_n e^{-2\sigma_n l} + D_n) \} \sin \sigma_n t + \frac{2}{\pi} \sum_{n=1}^{\infty} G(\alpha_n, t) F_n, \end{aligned} \quad (3.35)$$

$$\begin{aligned} \left(\frac{\pi}{2}\right)^{1/2} t^2 g_1(t) &= \frac{4ht^3}{(h^2 + t^2)^2} + \frac{2t^3 E_0}{3} - \sum_{n=1}^{\infty} (C_n + D_n e^{-2\sigma_n l}) \left( \frac{\sin \sigma_n t}{\sigma_n} - t \cos \sigma_n t \right) \\ &- \sum_{n=1}^{\infty} H(\alpha_n, t) E_n, \end{aligned} \quad (3.36)$$

and

$$\begin{aligned} \left(\frac{\pi}{2}\right)^{1/2} t^2 g_3(t) &= \frac{2t^3 E_0}{3} + \sum_{n=1}^{\infty} \{ 2\sigma_n l (A_n e^{-2\sigma_n l} - B_n) + (2\sigma_n l - 1) e^{-2\sigma_n l} C_n \\ &- (2\sigma_n l + 1) D_n \} \left( \frac{\sin \sigma_n t}{\sigma_n} - t \cos \sigma_n t \right) - \sum_{n=1}^{\infty} H(\alpha_n, t) E_n, \end{aligned} \quad (3.37)$$

where

$$G(\alpha_n t) = \left( 2 - \frac{\alpha_n I_0(\alpha_n)}{I_1(\alpha_n)} \right) \sinh \alpha_n t + \alpha_n t \cosh \alpha_n t, \quad (3.38)$$

and

$$H(\alpha_n, t) = \alpha_n t^2 \sinh \alpha_n t + \frac{I_0(\alpha_n)}{I_1(\alpha_n)} (\sinh \alpha_n t - \alpha_n t \cosh \alpha_n t). \quad (3.39)$$

The constants  $Q_1, Q_2$  in (3.34), (3.35) can be expressed in terms of  $M$  and the coefficient sequences  $\{A_n\} - \{F_n\}$  by means of the flux conservation relations (3.9), viz.

$$Q_1 = \frac{3M}{4} - \frac{6}{1+h^2} + 3 \sum_{n=1}^{\infty} \sigma_n^{-2} (A_n - B_n e^{-2\sigma_n l}) (\sigma_n \cos \sigma_n - \sin \sigma_n) + 3 \sum_{n=1}^{\infty} \left\{ \frac{I_0(\alpha_n)}{I_1(\alpha_n)} \cosh \alpha_n - \left( \frac{I_0(\alpha_n)}{\alpha_n I_1(\alpha_n)} + 1 \right) \sinh \alpha_n \right\} F_n, \quad (3.40)$$

$$Q_2 = -\frac{3M}{4} + 4E_0 l + 3 \sum_{n=1}^{\infty} \sigma_n^{-2} \left\{ (2\sigma_n l + 1) e^{-2\sigma_n l} A_n + (2\sigma_n l - 1) B_n + 2\sigma_n l (e^{-2\sigma_n l} C_n + D_n) \right\} (\sigma_n \cos \sigma_n - \sin \sigma_n) + 3 \sum_{n=1}^{\infty} \left\{ \frac{I_0(\alpha_n)}{I_1(\alpha_n)} \cosh \alpha_n - \left( \frac{I_0(\alpha_n)}{\alpha_n I_1(\alpha_n)} + 1 \right) \sinh \alpha_n \right\} F_n. \quad (3.41)$$

We now have available equations sufficient to express the functions  $j_1(t), j_3(t), g_1(t)$  and  $g_3(t)$  as linear combinations of the coefficients  $A_n$  through  $D_n$ , and the ultimate sets of linear equations for determining these coefficients are supplied by substituting for  $j_1$  through  $g_3$  in (3.26)–(3.29). Defining

$$\Theta_m = \sum_{s=1}^{\infty} J_0(\sigma_s) \Psi_i(s, n), \quad i = 0, 1, \quad (3.42)$$

these sets of equations take the form

$$\frac{1}{2} J_0^2(\sigma_m) (A_m + B_m e^{-2\sigma_m l}) + \sum_{n=1}^{\infty} \{M_{11}(m, n) A_n + M_{12}(m, n) B_n + M_{13}(m, n) C_n + M_{14}(m, n) D_n - E_{11}(m, n) \Theta_{1n} + E_{12}(m, n) \Theta_{0n}\} = U_{1m}, \quad (3.43)$$

$$\frac{1}{2} J_0^2(\sigma_m) (C_m - D_m e^{-2\sigma_m l}) + \sum_{n=1}^{\infty} \{M_{21}(m, n) A_n + M_{22}(m, n) B_n + M_{23}(m, n) C_n + M_{24}(m, n) D_n - E_{21}(m, n) \Theta_{1n} + E_{22}(m, n) \Theta_{0n}\} = U_{2m}, \quad (3.44)$$

$$\begin{aligned}
& \frac{1}{2}J_0^2(\sigma_m) \{(2\sigma_m l + 1)e^{-2\sigma_m l} A_m + (1 - 2\sigma_m l)B_m + \sigma_m l(e^{-2\sigma_m l} C_m - D_m)\} \\
& + \sum_{n=1}^{\infty} \{M_{31}(m, n)A_n + M_{32}(m, n)B_n + M_{33}(m, n)C_n + M_{34}(m, n)D_n \\
& + E_{11}(m, n)\Theta_{1n} + E_{12}(m, n)\Theta_{0n}\} = U_{3m},
\end{aligned} \tag{3.45}$$

$$\begin{aligned}
& \frac{1}{2}J_0^2(\sigma_m) \{2\sigma_m l(A_m e^{-2\sigma_m l} + B_m) + (2\sigma_m l - 1)e^{-2\sigma_m l} C_m + (2\sigma_m l + 1)D_m\} \\
& + \sum_{n=1}^{\infty} \{M_{41}(m, n)A_n + M_{42}(m, n)B_n + M_{43}(m, n)C_n + M_{44}(m, n)D_n \\
& + E_{21}(m, n)\Theta_{1n} + E_{22}(m, n)\Theta_{0n}\} = U_{4m},
\end{aligned} \tag{3.46}$$

all for  $m = 1, 2, \dots$ . The right members  $U_{im}$ ,  $i = 1, \dots, 4$ , of (3.43)–(3.46) are given by

$$\begin{aligned}
U_{1m} &= \frac{3}{2\pi\sigma_m^3} \left( M - \frac{8}{1+h^2} \right) (\sigma_m \cos \sigma_m - \sin \sigma_m) - \frac{4M}{\pi\sigma_m^2} J_0(\sigma_m) \\
&+ \frac{4}{\pi\sigma_m} \int_0^1 \frac{t(t^2 + 3h^2)}{(t^2 + h^2)^2} \sin \sigma_m t \, dt,
\end{aligned} \tag{3.47}$$

$$\begin{aligned}
U_{2m} &= -\frac{8M}{3\pi^2\sigma_m^4} \{-3\sigma_m \cos \sigma_m + (3 - \sigma_m^2) \sin \sigma_m\} - \frac{4h \sin \sigma_m}{\pi\sigma_m^2(1+h^2)} \\
&+ \int_0^1 \frac{(h^2 - t^2)}{(h^2 + t^2)^2} \cos \sigma_m t \, dt,
\end{aligned} \tag{3.48}$$

$$U_{3m} = -\frac{4M}{\pi\sigma_m^2} J_0(\sigma_m) + \frac{3M}{2\pi\sigma_m^3} (\sigma_m \cos \sigma_m - \sin \sigma_m), \tag{3.49}$$

and

$$U_{4m} = -\frac{8M}{3\pi^2\sigma_m^4} \{-3\sigma_m \cos \sigma_m + (3 - \sigma_m^2) \sin \sigma_m\}. \tag{3.50}$$

The remaining coefficients  $M_{ij}(m, n)$ ,  $i, j = 1, \dots, 4$ , and  $E_{ij}(m, n)$ ,  $i, j = 1, 2$ , are all functions of  $l$ ,  $\sigma_m$ ,  $\sigma_n$ ,  $\alpha_n$  and  $\alpha_m$ ; for reference they are recorded in the Appendix. It is of interest to note that only infinite summations are involved in (3.43)–(3.46), whereas in the semi-infinite-pore case [1] the coefficient matrices contain infinite integrations. Thus from the computational point of view the algebraic complexity of the truncated forms of (3.43)–(3.46) is somewhat off-set by the absence of numerical integrations.

When the Stokeslet is placed within the pore at  $z = -h$ ,  $0 < h < 2l$ , the velocity representations (3.1) and (3.10) need modifying, the form of  $\mathbf{v}^{\text{III}}$  (equation 3.5) remaining the same. In (3.1) the singular Stokeslet terms  $\mathbf{v}_0$  is now omitted, and we redefine  $\mathbf{v}_0$  to be



the velocity field produced by an axial Stokeslet placed at  $z = -h$  in an infinitely long fluid-filled circular cylinder of unit radius. Then [11] we have

$$\mathbf{v}_0 \cdot \mathbf{e} = \frac{\varrho(z + h)}{R_2^3} - \int_0^\infty k \{ \varrho F(k) I_0(k\varrho) - G(k) I_1(k\varrho) \} \sin k(z + h) dk, \quad (3.51)$$

$$\mathbf{v}_0 \cdot \mathbf{z} = \frac{2}{R_2} - \frac{\varrho^2}{R_2^3} - \int_0^\infty [F(k) \{ \varrho k I_1(k\varrho) + 2 I_0(k\varrho) \} - k G(k) I_0(k\varrho)] \cos k(z + h) dk, \quad (3.52)$$

where

$$F(k) = -2 \{ K_1(k) I_1(k) + K_0(k) I_2(k) \} / \pi \Delta(k), \quad (3.53)$$

$$G(k) = -2 / \pi k \Delta(k), \quad (3.54)$$

and the associated pressure field is

$$p_0 = \frac{2\mu(z + h)}{R_2^3} - 2\mu \int_0^\infty k F(k) I_0(k\varrho) \sin k(z + h) dk. \quad (3.55)$$

The velocity and pressure  $\mathbf{v}^{\text{II}}$  and  $p^{\text{II}}$  in the pore are now taken to be the forms (3.10) and (3.11) with  $\mathbf{v}_0$  and  $p_0$  added to the right-hand sides; the definitions (3.12) of the various constituent harmonic functions remain the same. The computations leading to (3.43) through (3.46) can now be repeated, resulting in a modified system of four coupled infinite sets of linear equations for the coefficient sequences  $\{A_n\} - \{D_n\}$ . The left members of these equations are identical to (3.43) through (3.46), but the right members are replaced by functions  $\tilde{U}_{im}$ ,  $i = 1, \dots, 4$ ,  $m = 1, 2, \dots$ , considerably more complex than the  $U_{im}$  of (3.47)–(3.50). To avoid over elaboration they are not recorded here, but full details may be had from the authors.

#### 4. Drag on a small sedimenting particle

Suppose that a small sedimenting particle is situated on the axis of the pore at a point  $P$  with  $z$ -coordinate  $h$  ( $> 0$ ) or  $-h$  depending on whether the particle is in the half-space  $z > 0$  or the pore. We assume that the particle translates along the pore axis parallel to a principal axis of resistance with a velocity  $U_0 \mathbf{z}$ ; denote by  $-F \mathbf{z}$  and  $-F_\infty \mathbf{z}$  the viscous drag forces on the particle for motion in the bounded and everywhere infinite fluid. As in Section 2 the pore radius is  $c$  in physical units with  $b = ch$ , and  $a$  is a typical particle dimension. For any position of the particle let  $\mathbf{v}^*$  be the regular part of the velocity field, in the fluid region containing the particle, which obtains if the particle is replaced by an axial Stokeslet of unit strength. According to Brenner [2] when there is a volume flux  $M$  of fluid through the pore  $F$  is given by

$$\frac{F_\infty}{F} = 1 - \frac{C_2 F_\infty}{8\pi\mu c U_0} \left( 1 - \frac{M w_z(P)}{U_0} \right) (1 + O(a/L)^2), \quad (4.1)$$

where  $L = \max(b, c)$  and  $w_z(P)$  is the axial fluid speed at  $P$  appropriate to the problem of a unit flux of fluid through the pore in the absence of the particle. The drag factor  $C_2$  in (4.1) is defined by

$$C_2 = -\mathbf{v}^*(P) \cdot \mathbf{z} \quad (4.2)$$

where here  $\mathbf{v}^*(P)$  pertains to the case  $M = 0$ , a situation in which the error in (4.1) can be shown ([2], [12]) to be  $O(a/L)^3$ .

In order to evaluate  $C_2$ , suppose first that the particle is in  $z > 0$ . Then  $\mathbf{v}^*$  follows from (3.1) and (3.3) by omitting the terms in  $\mathbf{v}_0$  containing inverse powers of  $R_1$ . From (3.7) and (3.8)  $C_2$  is now expressed in terms of  $j_1(t)$  and  $g_1(t)$  as

$$C_2 = \frac{3}{2h} - \int_0^1 \frac{t}{(t^2 + h^2)^2} \left\{ (t^2 + 3h^2)j_1(t) + 2h \left( \frac{2}{\pi} \right)^{1/2} t^2 g_1(t) \right\} dt, \quad (4.3)$$

where  $j_1(t)$ ,  $g_1(t)$  are found from (3.34), (3.36) and (3.40). The appropriate equations for the coefficient sequences  $\{A_n\} - \{D_n\}$  are obtained by setting  $M = 0$  in the right-hand sides (3.47)–(3.50) of equations (3.43)–(3.46), the resulting linear system being solved by truncation. For the particle inside the pore at  $z = -h$ ,  $0 < h < 2l$ , the relevant velocity component in (4.2) follows as the regular part of (3.10) augmented by the field  $\mathbf{v}_0$  with components (3.51) and (3.52). There results

$$\begin{aligned} C_2 = & F_0 - \int_0^\infty \{2F(k) - kG(k)\} dk \\ & - \sum_{n=1}^\infty \{(\sigma_n h + 1)e^{-\sigma_n h} A_n - (\sigma_n h - 1)e^{-\sigma_n(2l-h)} B_n + \sigma_n h(C_n e^{-\sigma_n h} - D_n e^{-\sigma_n(2l-h)})\} \\ & - \sum_{n=1}^\infty \{(2E_n - \alpha_n H_n) \cos \alpha_n h - (2F_n + \alpha_n G_n) \sin \alpha_n h\}, \end{aligned} \quad (4.4)$$

where  $F_0$  follows from (3.13) and (3.21) and  $F(k)$ ,  $G(k)$  are defined in (3.53), (3.54). The equations for  $\{A_n\} - \{D_n\}$  are (3.43)–(3.46) with right-members obtained by setting  $M = 0$  in the  $\tilde{U}_{im}$  of Section 3, and are again solved by truncation.

One further quantity of interest is the additional pressure drop,  $\Delta p = p_{-\infty} - p_\infty$ , due to the presence of the sedimenting particle. For the particle in the half-space chamber  $z > 0$ , and  $M = 0$ , we have from (3.40) and (3.41) that

$$\begin{aligned} -\frac{\Delta p}{2\mu} = & Q_2 - Q_1 \\ = & \frac{6}{1 + h^2} + 4E_0 l + 3 \sum_{n=1}^\infty \sigma_n^{-2} (\sigma_n \cos \sigma_n - \sin \sigma_n) [\{(2\sigma_n l + 1)e^{-2\sigma_n l} - 1\} A_n \\ & + \{2\sigma_n l - 1 + e^{-2\sigma_n l}\} B_n + 2\sigma_n l (C_n e^{-2\sigma_n l} + D_n)]. \end{aligned} \quad (4.5)$$

For the particle within the pore the pressure drop is similarly found as

$$\begin{aligned}
 -\frac{\Delta p}{2\mu} = & 3 \left\{ \frac{1}{1 + (h - 2l)^2} + \frac{1}{1 + h^2} \right\} + 4E_0 l \\
 & + 3 \sum_{n=1}^{\infty} \sigma_n^{-2} (\sigma_n \cos \sigma_n - \sin \sigma_n) [\{(2\sigma_n l + 1)e^{-2\sigma_n l} - 1\}A_n \\
 & + \{2\sigma_n l - 1 + e^{-2\sigma_n l}\}B_n + 2\sigma_n l(C_n e^{-2\sigma_n l} + D_n)] \\
 & - 6 \int_0^{\infty} \{\sinh kF(k) - k^{-1}(k \cosh k - \sinh k)G(k)\} \sin lk \cos (h - l)k \, dk.
 \end{aligned}
 \tag{4.6}$$

The results of the detailed calculations in the zero-flux case, using the numerical techniques described in Section 2, are illustrated in Figs 3, 4 and 5. Figure 3 gives the variation of the drag factor with particle position for various pore lengths; observe that for a pore length of about 2 pore radii the drag-factor curve is virtually indistinguishable from that for a semi-infinite pore for particle positions with  $z_p$  in the range  $-1 \leq z_p < \infty$ . The maximum drag factor occurs when the particle is at the mid-point of the pore, and Figure 4 shows the variation of this maximum with pore length; the horizontal asymptote is the semi-infinite length pore value of  $C_2$ , namely 2.806. Figure 5 provides curves of additional pressure drop against particle position for various pore lengths. In Figs. 3 and 5

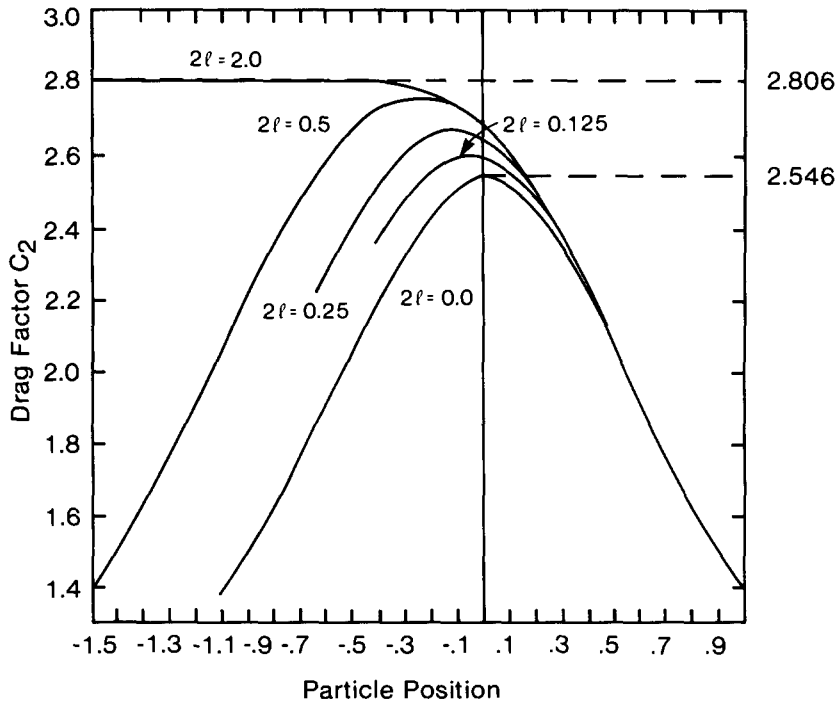


Fig. 3. The drag factor  $C_2$  plotted against particle position for various pore lengths (zero-flux case).

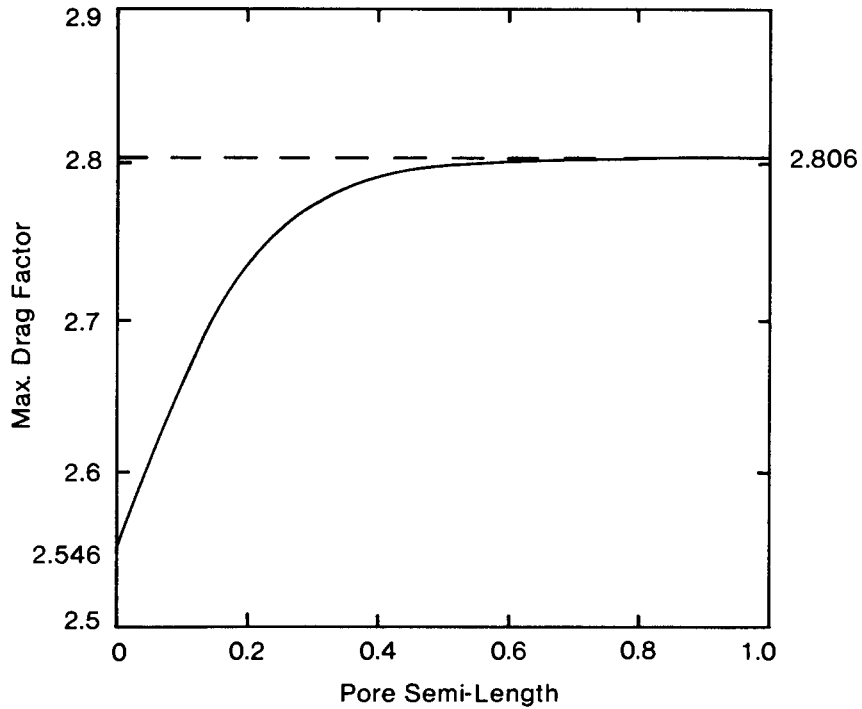


Fig. 4. The maximum drag factor (with the particle at the centre of the pore) plotted as a function of pore semi-length.

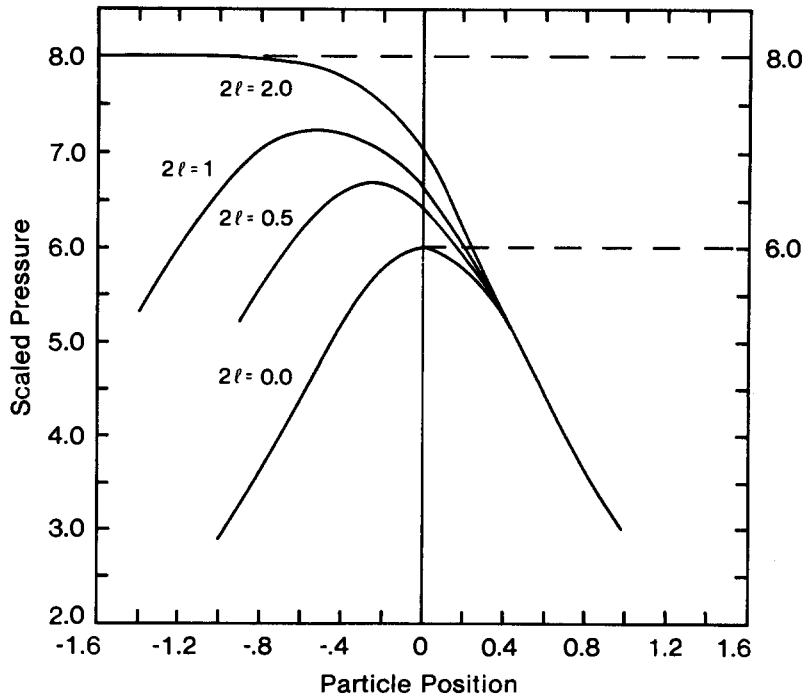


Fig. 5. The additional pressure drop (zero-flux case) due to the presence of the particle plotted against particle position for various pore lengths.

the zero-length pore results are calculated from the formulae

$$C_2' = \frac{1}{\pi} \left( \frac{3}{h} \tan^{-1} h + \frac{3}{1+h^2} + \frac{2}{(1+h^2)^2} \right), \quad \frac{\Delta p'}{2\mu} = -\frac{6}{1+h^2}, \quad (4.7)$$

quoted in [1].

We now turn to the case in which there is a non-zero flux through the pore. As noted earlier the drag calculation using (4.1) requires only the further knowledge of  $w_z(P)$ , the axial fluid speed, with unit flux, at the particle position  $P$  in the absence of the particle. The appropriate results can be obtained by setting  $M = 1$  and omitting from the right-hand sides of the systems of linear equations all terms involving  $h$  (or, equivalently, letting  $h \rightarrow \infty$ ). However the coordinate system used in Section 3, whilst optimizing the difficult Stokeslet calculations, does not exploit the symmetry of the singularity-free problem about the mid-plane of the pore. Therefore we give a reformulation of this problem with the origin of coordinates  $O$  relocated at the centre of the pore. The membrane faces are now  $z = \pm l$ ,  $\varrho > 1$ , and it is only necessary to consider the regions  $z \geq l$  (I) and the half-pore  $0 \leq z \leq l$ ,  $0 \leq \varrho \leq 1$  (II), continuation of the solution into the remaining fluid regions being effected by noting the even and odd parities of  $\mathbf{v} \cdot \mathbf{z}$  and  $\mathbf{v} \cdot \boldsymbol{\varrho}$  with respect to  $z$ .

Appropriate velocity and pressure representations in the two fluid regions are as follows, all constituent functions being axially symmetric harmonics. In  $z > l$ ,

$$\mathbf{v}^I = (z - l)\nabla\phi - \phi\mathbf{z} + (z - l)\nabla\psi - \psi\mathbf{z} + \nabla\tilde{\omega}, \quad \psi = \frac{\partial\tilde{\omega}}{\partial z}, \quad (4.8)$$

$$p^I = p_\infty + 2\mu \left( \frac{\partial\phi}{\partial z} + \frac{\partial\psi}{\partial z} \right), \quad (4.9)$$

where

$$\phi(\varrho, z) = - \int_0^1 j(t) \left\{ \int_0^\infty \sin \alpha t J_0(\alpha\varrho) e^{-\alpha(z-l)} d\alpha \right\} dt, \quad (4.10)$$

$$\frac{\partial\tilde{\omega}}{\partial\varrho} = - \int_0^1 t^{3/2} g(t) \left\{ \int_0^\infty \alpha^{1/2} J_{3/2}(\alpha t) J_1(\alpha\varrho) e^{-\alpha(z-l)} d\alpha \right\} dt. \quad (4.11)$$

In  $0 \leq z \leq l$ , (3.10) and (3.11) are used with the following redefinitions of the harmonic functions  $U, \dots, Y$ :

$$U = \sum_{n=1}^\infty A_n (e^{\sigma_n(z-l)} + e^{-\sigma_n(z+l)}) J_0(\sigma_n\varrho),$$

$$V = \sum_{n=1}^\infty B_n (e^{\sigma_n(z-l)} + e^{-\sigma_n(z+l)}) J_0(\sigma_n\varrho),$$

$$\begin{aligned}
 W &= \sum_{n=1}^{\infty} \sigma_n^{-1} B_n (e^{\sigma_n(z-l)} - e^{-\sigma_n(z+l)}) J_0(\sigma_n \varrho), \\
 X &= \sum_{n=1}^{\infty} E_n I_0(\alpha_n \varrho) \cos \alpha_n z, \quad Y = \sum_{n=1}^{\infty} F_n I_0(\alpha_n \varrho) \sin \alpha_n z.
 \end{aligned}
 \tag{4.12}$$

Imposition of the no-slip condition on the pore walls and the velocity and stress matching across  $z = l, 0 \leq \varrho \leq 1$ , now produce coupled infinite sets of linear equations for  $\{A_n\}$  and  $\{B_n\}$ , as follows. Define

$$\begin{aligned}
 \Theta_n &= 2 \sum_{s=1}^{\infty} \frac{\sigma_s J_0(\sigma_s)}{(\sigma_s^2 + \alpha_n^2)^2} [\sigma_s \{l(\sigma_s^2 + \alpha_n^2)(1 + e^{-2\sigma_s l}) - 2\sigma_s(1 - e^{-2\sigma_s l})\} A_s \\
 &\quad + \{\sigma_s l(\sigma_s^2 + \alpha_n^2)(1 + e^{-2\sigma_s l}) - (\sigma_s^2 - \alpha_n^2)(1 - e^{-2\sigma_s l})\} B_s];
 \end{aligned}
 \tag{4.13}$$

then

$$\begin{aligned}
 &\frac{1}{2} J_0^2(\sigma_m) [\{1 - \sigma_m l + (\sigma_m l + 1)e^{-2\sigma_m l}\} A_m + \sigma_m l(1 - e^{-2\sigma_m l}) B_m] \\
 &\quad + \sum_{n=1}^{\infty} \{M'_{11}(m, n) A_n + M'_{12}(m, n) B_n + E_{12}(m, n) \Theta_n\} \\
 &= \frac{3}{2\pi\sigma_m^3} (\sigma_m \cos \sigma_m - \sin \sigma_m) - \frac{4J_0(\sigma_m)}{\pi\sigma_m^2},
 \end{aligned}
 \tag{4.14}$$

and

$$\begin{aligned}
 &\frac{1}{2} J_0^2(\sigma_m) [\sigma_m l(1 + e^{-2\sigma_m l}) A_m + \{\sigma_m l + 1 + (\sigma_m l - 1)e^{-2\sigma_m l}\} B_m] \\
 &\quad + \sum_{n=1}^{\infty} \{M'_{21}(m, n) A_n + M'_{22}(m, n) B_n + E_{22}(m, n) \Theta_n\} \\
 &= -\frac{1}{\pi} \tau(\sigma_m), \quad m = 1, 2, \dots
 \end{aligned}
 \tag{4.15}$$

In (4.14) and (4.15),  $\tau(\sigma_m), E_{12}(m, n), E_{22}(m, n)$  are defined in the Appendix and the remaining coefficients are (with  $\kappa(\sigma_m, \sigma_n)$  also given in the Appendix)

$$\begin{aligned}
 M'_{11}(m, n) &= \frac{4J_0(\sigma_m) J_0(\sigma_n)}{\sigma_m^2 \sigma_n l} \{\sigma_n l - 2 + (\sigma_n l + 2)e^{-2\sigma_n l}\} \\
 &\quad + \{\sigma_n l - 1 + (\sigma_n l + 1)e^{-2\sigma_n l}\} \kappa(\sigma_m, \sigma_n),
 \end{aligned}
 \tag{4.16}$$

$$M'_{12}(m, n) = M'_{11}(m, n) + (1 - e^{-2\sigma_n l}) \{4(\sigma_m^2 \sigma_n l)^{-1} J_0(\sigma_m) J_0(\sigma_n) + \kappa(\sigma_m, \sigma_n)\}, \tag{4.17}$$

$$M'_{21}(m, n) = \frac{2\sigma_n l}{\pi\sigma_m} (1 - e^{-2\sigma_n l}) E_{25}(m, n) + \frac{J_0(\sigma_n)}{\sigma_n l} \tau(\sigma_m) \{\sigma_n l - 2 + (\sigma_n l + 2)e^{-2\sigma_n l}\}, \quad (4.18)$$

where  $E_{25}(m, n)$  is given by (A18), and

$$M'_{22}(m, n) = \frac{2}{\pi\sigma_m} \{\sigma_n l + 1 - (\sigma_n l - 1)e^{-2\sigma_n l}\} E_{25}(m, n) + \frac{J_0(\sigma_n)}{\sigma_n l} \tau(\sigma_m) \{\sigma_n l - 1 + (\sigma_n l + 1)e^{-2\sigma_n l}\}. \quad (4.19)$$

The coefficients  $E_0, F_0$  in (3.10) are given in terms of  $\{A_n\}, \{B_n\}$  by

$$E_0 = -\frac{2}{\pi} - \frac{2}{l} \sum_{n=1}^{\infty} \sigma_n^{-1} J_0(\sigma_n) [\{\sigma_n l - 2 + (\sigma_n l + 2)e^{-2\sigma_n l}\} A_n + \{\sigma_n l - 1 + (\sigma_n l + 1)e^{-2\sigma_n l}\} B_n], \quad (4.20)$$

with

$$F_0 = \frac{1}{\pi} - \frac{1}{2} E_0. \quad (4.21)$$

In order to evaluate  $w_z(P)$  at  $P(\varrho = 0, z = h)$ , suppose first that  $h > l$ ; then from (4.8), (4.10) and (4.11) we find that

$$w_z(P) = \int_0^1 \frac{t}{\{t^2 + (h-l)^2\}^2} \left[ \{3(h-l)^2 + t^2\} j(t) + 2 \left(\frac{2}{\pi}\right)^{1/2} (h-l)t^2 g(t) \right] dt, \quad (4.22)$$

Similarly, for  $0 < h < l$ , (3.10) and (4.12) provide the expression

$$w_z(P) = F_0 + \sum_{n=1}^{\infty} [e^{\sigma_n(h-l)} \{(\sigma_n h - 1)A_n + \sigma_n h B_n\} - e^{-\sigma_n(h+l)} \{(\sigma_n h + 1)A_n + \sigma_n h B_n\}] + \sum_{n=1}^{\infty} (-2E_n + \alpha_n F_n) \cos \alpha_n h. \quad (4.23)$$

The pressure drop between  $z = -\infty$  and  $z = +\infty$  is  $\Delta p = p_{-\infty} - p_{\infty}$ , where

$$-\frac{\Delta p}{2\mu} = -\frac{3}{2} + 4E_0 l - 6 \sum_{n=1}^{\infty} \sigma_n^{-2} (\sin \sigma_n - \sigma_n \cos \sigma_n) \times [\{\sigma_n l - 1 + (\sigma_n l + 1)e^{-2\sigma_n l}\} A_n + \sigma_n l e^{-2\sigma_n l} B_n]. \quad (4.24)$$

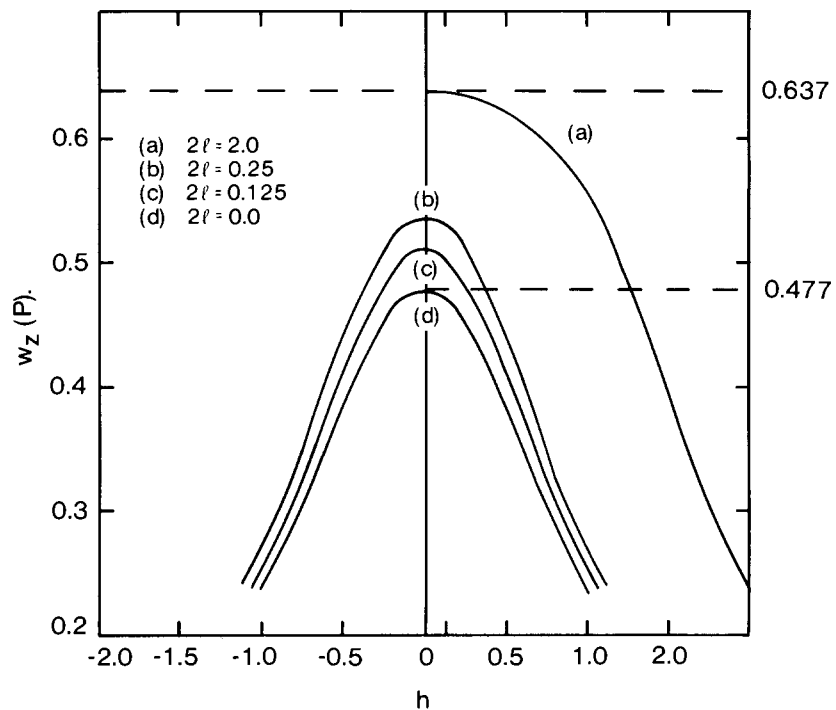


Fig. 6. Graphs of  $w_z(P)$  as a function of position for various pore lengths (unit flux through the pore).

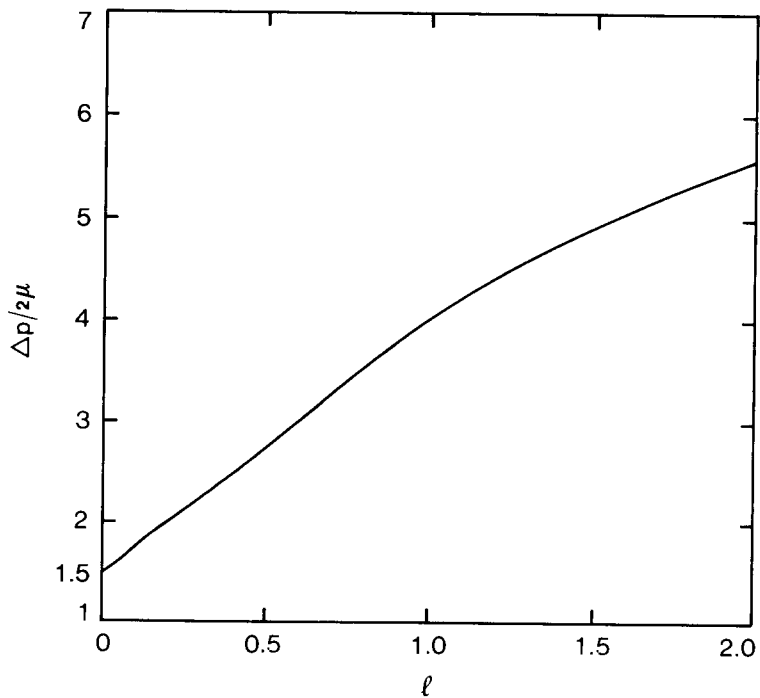


Fig. 7. The scaled pressure  $\Delta p / 2\mu$  plotted against pore semi-length (unit flux through the pore).



Figure 6 gives a plot of the axial flow speed  $w_z(P)$  as a function of  $h$  and various pore lengths, there being unit flux through the pore. Also illustrated in Fig. 6 is the corresponding curve for an infinitely thin membrane, for which

$$w'_z(P) = \frac{3}{2\pi(h^2 + 1)}. \quad (4.25)$$

Figure 7 shows the scaled pressure drop,  $\Delta P/2\mu$ , as a function of pore semi-length. As a check on our analyses the results computed from (4.24) were compared with those obtained from (4.5) using a large value of  $h$  ( $\sim 50$ ) and very satisfactory agreement to three decimal places was obtained for pore lengths small compared with  $h$ . The results also agree with those of Dagan et al. [4], but it is noteworthy that the method given here involves a doubly-infinite set of unknown coefficients, whereas in [4] a four-fold infinity has to be found.

## 5. Conclusion

The results illustrated in Fig. 6, together with those derived earlier for the singularity-driven zero-flux flow, provide via equation (4.1) a complete description of the approximate drag experienced by an axially located small particle sedimenting through a circular pore in a membrane of finite thickness. If the particle is also rotating about the pore axis then the couple approximation is supplied by the formulae of Section 2. These flows are assumed to be sufficiently slow for the quasi-steady Stokes approximation to be valid, and the computations bridge the gap between the infinitely thin membrane model of Davis et al. [3] and the semi-infinite pore used in [1]. Both these approximations are valuable, and the latter is very accurate for pore lengths of the order of two pore radii or greater.

The algebraic analysis of the finite-length pore model when the flow is driven by an axial point force (Stokeslet) is complicated, and the configuration probably represents the limit of what is practicable using potential theoretic methods. Such procedures are most suited for pores of circular cross-section, and for other geometries numerical methods are to be preferred. To this end the present authors are investigating the use of the method of subareas with a view to eventually discussing, for example, pores of elliptical or rectangular cross-section.

Some progress can be made with potential methods in non-axially symmetric configurations. In particular the problem of a shear flow along the wall of the membrane, the pore being of semi-infinite length, can be reduced to the solution of four simultaneous infinite sets of linear equations, and results will be reported elsewhere. Replacing the shear flow by a rotlet or Stokeslet with axis oriented parallel to the membrane wall is a further problem which can be formulated in principle, but the super-complexity of the algebra makes this a daunting undertaking. (See [13] for the solution of these asymmetric problems when the membrane is infinitely thin.)

## Acknowledgement

One of the authors (I.M.W.) acknowledges with thanks the receipt of a Research Studentship from the Science and Engineering Research Council during the time in which this work was carried out.

**Appendix**

In this Appendix we list the various coefficients  $M_{ij}(m, n)$  and  $E_{ij}(m, n)$  appearing in the linear systems (3.43)–(3.46). Define  $\kappa(\sigma_m, \sigma_n)$  and  $\tau(\sigma_m)$  by

$$\begin{aligned} \kappa(\sigma_m, \sigma_n) = & \frac{1}{\pi\sigma_m^3\sigma_n^2} \left[ 6(\sigma_m \cos \sigma_m - \sin \sigma_m)(\sigma_n \cos \sigma_n - \sin \sigma_n) \right. \\ & \left. - \sigma_m^2\sigma_n^2 \left\{ \frac{\sin(\sigma_m - \sigma_n)}{\sigma_m - \sigma_n} - \frac{\sin(\sigma_m + \sigma_n)}{\sigma_m + \sigma_n} \right\} \right], \end{aligned} \quad (\text{A1})$$

$$\tau(\sigma_m) = \frac{8}{3\pi\sigma_m^4} \{-3\sigma_m \cos \sigma_m + (3 - \sigma_m^2) \sin \sigma_m\}.$$

Then the coefficients in (3.43) are

$$M_{11}(m, n) = \frac{4J_0(\sigma_m)J_0(\sigma_n)}{l\sigma_m^2\sigma_n} \{(1 + \sigma_n l)e^{-2\sigma_n l} - 1\} - \kappa(\sigma_m, \sigma_n), \quad (\text{A2})$$

$$M_{12}(m, n) = \frac{4J_0(\sigma_m)J_0(\sigma_n)}{l\sigma_m^2\sigma_n} \{e^{-2\sigma_n l} + \sigma_n l - 1\} + \kappa(\sigma_m, \sigma_n)e^{-2\sigma_n l}, \quad (\text{A3})$$

$$M_{13}(m, n) = \frac{2J_0(\sigma_m)J_0(\sigma_n)}{l\sigma_m^2\sigma_n} \{(1 + 2\sigma_n l)e^{-2\sigma_n l} - 1\}, \quad (\text{A4})$$

$$M_{14}(m, n) = \frac{2J_0(\sigma_m)J_0(\sigma_n)}{l\sigma_m^2\sigma_n} \{2\sigma_n l - 1 + e^{-2\sigma_n l}\}, \quad (\text{A5})$$

$$\begin{aligned} E_{11}(m, n) = & -\frac{2I_1(\alpha_n)}{\pi l \sigma_m \alpha_n \Delta(\alpha_n)} \left\{ \left( 2 - \frac{\alpha_n I_0(\alpha_n)}{I_1(\alpha_n)} \right) E_{13}(m, n) + \alpha_n E_{14}(m, n) \right\} \\ & - \frac{6(\sigma_m \cos \sigma_m - \sin \sigma_m)}{\pi l \sigma_m^3 \alpha_n^2 \Delta(\alpha_n)} [\{\alpha_n I_1(\alpha_n) + I_0(\alpha_n)\} \sinh \alpha_n - \alpha_n I_0(\alpha_n) \cosh \alpha_n], \end{aligned} \quad (\text{A6})$$

$$E_{12}(m, n) = \frac{2\sigma_m^2 J_0(\sigma_m) I_1^2(\alpha_n)}{l(\sigma_m^2 + \alpha_n^2)^2 \Delta(\alpha_n)}. \quad (\text{A7})$$

where

$$E_{13}(m, n) = (\alpha_n \cosh \alpha_n \sin \sigma_m - \sigma_m \sinh \alpha_n \cos \sigma_m)/(\sigma_m^2 + \alpha_n^2), \quad (\text{A8})$$

$$\begin{aligned} E_{14}(m, n) = & (\alpha_n \sinh \alpha_n \sin \sigma_m - \sigma_m \cosh \alpha_n \cos \sigma_m)/(\sigma_m^2 + \alpha_n^2) \\ & - \{(\alpha_n^2 - \sigma_m^2) \cosh \alpha_n \sin \sigma_m - 2\sigma_m \alpha_n \sinh \alpha_n \cos \sigma_m\}/(\sigma_m^2 + \alpha_n^2)^2. \end{aligned} \quad (\text{A9})$$

In equation (3.44) the coefficients are

$$M_{21}(m, n) = \frac{J_0(\sigma_n)}{\sigma_n l} \{(1 + \sigma_n l)e^{-2\sigma_n l} - 1\} \tau(\sigma_m), \quad (\text{A10})$$

$$M_{22}(m, n) = \frac{J_0(\sigma_n)}{\sigma_n l} \{e^{-2\sigma_n l} - 1 + \sigma_n l\} \tau(\sigma_m), \quad (\text{A11})$$

$$M_{23}(m, n) = \frac{J_0(\sigma_n)}{2\sigma_n l} \{(1 + 2\sigma_n l)e^{-2\sigma_n l} - 1\} \tau(\sigma_m) + \frac{2}{\pi\sigma_m} E_{25}(m, n), \quad (\text{A12})$$

$$M_{24}(m, n) = \frac{J_0(\sigma_n)}{2\sigma_n l} \{e^{-2\sigma_n l} - 1 + 2\sigma_n l\} \tau(\sigma_m) + \frac{2}{\pi\sigma_m} E_{25}(m, n)e^{-2\sigma_n l}, \quad (\text{A13})$$

$$E_{21}(m, n) = \frac{2\alpha_n \sigma_m J_0(\sigma_m) I_1^2(\alpha_n)}{l(\sigma_m^2 + \alpha_n^2)^2 \Delta(\alpha_n)} = \alpha_n \sigma_m^{-1} E_{12}(m, n), \quad (\text{A14})$$

$$E_{22}(m, n) = \frac{2}{\pi l \sigma_m \Delta(\alpha_n)} \{E_{23}(m, n) I_1(\alpha_n) - E_{24}(m, n) I_0(\alpha_n)\}, \quad (\text{A15})$$

where

$$\begin{aligned} E_{23}(m, n) = & \frac{1}{\sigma_m(\alpha_n^2 + \sigma_m^2)} \{ \alpha_n \cosh \alpha_n (\sin \sigma_m - \sigma_m \cos \sigma_m) \\ & - \sigma_m \sinh \alpha_n (\cos \sigma_m + \sigma_m \sin \sigma_m) \} \\ & + \frac{(\alpha_n^2 - \sigma_m^2) \sinh \alpha_n \cos \sigma_m + 2\alpha_n \sigma_m \cosh \alpha_n \sin \sigma_m}{(\alpha_n^2 + \sigma_m^2)^2}, \end{aligned} \quad (\text{A16})$$

$$E_{24}(m, n) = \frac{\sin \sigma_m \sinh \alpha_n}{\sigma_m \alpha_n} - \frac{(\sigma_m \sin \sigma_m \cosh \alpha_n + \alpha_n \cos \sigma_m \sinh \alpha_n)}{\sigma_m^2 + \alpha_n^2} \quad (\text{A17})$$

and

$$E_{25}(m, n) = \frac{\sin(\sigma_n + \sigma_m)}{2(\sigma_n + \sigma_m)} + \frac{\sin(\sigma_n - \sigma_m)}{2(\sigma_n - \sigma_m)} - \frac{\sin \sigma_m \sin \sigma_n}{\sigma_m \sigma_n}. \quad (\text{A18})$$

In (3.45) the remaining coefficients are

$$M_{31}(m, n) = M_{11}(m, n) + \{1 + (1 + 2\sigma_n l)e^{-2\sigma_n l}\} \kappa(\sigma_m, \sigma_n), \quad (\text{A19})$$

$$M_{32}(m, n) = M_{12}(m, n) + \{2\sigma_n l - 1 - e^{-2\sigma_n l}\} \kappa(\sigma_m, \sigma_n), \quad (\text{A20})$$

$$M_{33}(m, n) = M_{13}(m, n) + 2\sigma_n l e^{-2\sigma_n l} \kappa(\sigma_m, \sigma_n), \quad (\text{A21})$$

and

$$M_{34}(m, n) = M_{14}(m, n) + 2\sigma_n l \kappa(\sigma_m, \sigma_n). \quad (\text{A22})$$

Finally in (3.46) we have:

$$M_{41}(m, n) = M_{21}(m, n) - \frac{4l\sigma_n e^{-2\sigma_n l}}{\pi\sigma_m} E_{25}(m, n), \quad (\text{A23})$$

$$M_{42}(m, n) = M_{22}(m, n) + \frac{4l\sigma_n}{\pi\sigma_m} E_{25}(m, n), \quad (\text{A24})$$

$$M_{43}(m, n) = M_{23}(m, n) - \frac{2}{\pi\sigma_m} \{1 + (2\sigma_n l - 1)e^{-2\sigma_n l}\} E_{25}(m, n), \quad (\text{A25})$$

and

$$M_{44}(m, n) = M_{24}(m, n) + \frac{2}{\pi\sigma_m} \{1 + 2\sigma_n l - e^{-2\sigma_n l}\} E_{25}(m, n). \quad (\text{A26})$$

## References

1. R. Shail and B.A. Packham, Some potential problems associated with the sedimentation of a small particle into a semi-infinite fluid-filled pore, *IMA J. Appl. Math.* 37 (1986) 37–66.
2. H. Brenner, Effect of finite boundaries on the Stokes resistance of an arbitrary particle, *J. Fluid Mech.* 12 (1962) 35–48.
3. A.M.J. Davis, M.E. O'Neill and H. Brenner, Axisymmetric Stokes flows due to a rotlet or Stokeslet near a hole in a plane wall: filtration flows, *J. Fluid Mech.* 103 (1981) 183–205.
4. Z. Dagan, S. Weinbaum and R. Pfeffer, An infinite-series solution for creeping motion through an orifice of finite length, *J. Fluid Mech.* 115 (1982) 505–523.
5. L.M. Keer, A class of non-symmetrical punch and crack problems, *Q. Jl. Mech. Appl. Math.* 17 (1964) 420–436.
6. H. Brenner, Slow viscous rotation of an axisymmetric body within a cylinder of finite length, *Appl. Sci. Res.* A13 (1964) 81–120.
7. M.R. Hestenes and E. Stiefel, Method of conjugate gradients for solving linear systems, *J. Res. Nat. Bur. Standards* 49 (1952) 404–436.
8. D. Shanks, Non-linear transformations of divergent and slowly convergent sequences, *J. Math. Phys.* 34 (1955) 1–42.
9. A.E. Green and W.A. Zerna, *Theoretical Elasticity*, Oxford, Clarendon Press (1954).
10. I.N. Sneddon, *Mixed Boundary Value Problems in Potential Theory*, Amsterdam, North Holland (1966).
11. R.M. Sonshine, R.C. Cox and H. Brenner, The Stokes translation of a particle of arbitrary shape along the axis of a circular cylinder filled to a finite depth with viscous liquid I, *Appl. Sci. Res.* 16 (1966) 273–300.
12. W.E. Williams, Boundary effects in Stokes flow, *J. Fluid Mech.* 24 (1966) 285–291.
13. R. Shail and B.A. Packham, Some asymmetric Stokes flow problems, *J. Engng. Mathematics* 21 (1987) 331–348.